Biofilm 2 (2020) 100016

Contents lists available at ScienceDirect

Biofilm

journal homepage: www.elsevier.com/locate/bioflm

Widespread cryptic viral infections in lotic biofilms

Alexandra T. Payne [a], Abigail J. Davidson [a], Jinjun Kan [b], Marc Peipoch [b], Raven Bier [b], Kurt Williamson [a,*]

[a] The College of William & Mary, Williamsburg, VA, 23185, USA
[b] Stroud Water Research Center, 970 Spencer Rd, Avondale, PA, 19311, USA

ARTICLE INFO

Keywords:
Virus
Phage
Prophage
Induction
Stream
Lotic
Benthic
TEM
PCR
Microbial ecology

ABSTRACT

Viruses have important impacts on aquatic microbial ecology and have been studied at length in the global ocean. However, the roles of bacteriophages in lotic ecosystems, particularly in benthic biofilms, have been largely under-studied. The main goals of this work were to determine whether viruses are consistent members of natural benthic biofilm communities of freshwater streams; whether temperate phages are present and active in such biofilms; and whether community profiling approaches like RAPD-PCR can be adapted to characterize biofilm virus communities. Results from both field and laboratory experiments suggest that viruses are consistent members of lotic biofilm communities. Interestingly, prophage induction was statistically significant but only a small percentage of the total bacterial population appeared to harbor prophage or engaged in induction. Finally, while the use of RAPD-PCR for the community level profiling of biofilm viral communities suggests temporal change in response to biofilm maturity, further refinements are required for broad-scale quantitative application.

Introduction

Viruses are the most abundant biological entities in aquatic systems, and indeed, on the planet [1–3]. In most aquatic ecosystems, viral abundance exceeds bacterial abundance by an order of magnitude [4]. Given their high abundances, viruses have significant impacts on population-, community-, and ecosystem-level processes including top-down control of bacterial abundance [2], maintenance of microbial community composition [2,5], and nutrient fluxes through food webs [6–10]. In addition, viruses exert important influence over host evolution through selection and gene transfer [11].

While most of our understanding of viral impacts assume lytic interactions between virus and host, other viral replication strategies are possible. Bacteriophages (viruses that infect bacteria) may replicate through one of four known modes, including lytic [12], lysogenic [13], pseudolysogenic [14], and chronic infections [15]. The focus of the present study is lysogenic replication, which involves suppression of lytic functions by the phage. Once inside the cell, the phage genome is stably maintained as an integrated part of the bacterial chromosome (prophage), or as an extrachromosomal element, in a state known as lysogeny. Subsequent environmental signals that cause physiological stress (the most clearly understood signal is DNA damage) can induce suppressed lytic functions to resume, releasing phage progeny through cell lysis [16,17]. Lysogeny is important because it serves as an efficient mechanism for introducing new genes into bacterial hosts and provides a long-term survival strategy to phages [18–22]. To understand the relative importance of lysogeny in a given environment, previous studies have used the rate of prophage induction in sampled bacterial communities as a proxy measure [23]. Prophage induction has been used to assess lysogeny in many different environments including deep sea hydrothermal vents [24], soils [25], marine sediments [26], and coastal water samples [27–30]. However, the role of temperate phage in freshwater ecosystems, particularly in lotic ecosystems such as streams, remain understudied [10,24].

Lotic ecosystems (moving freshwaters) alter the surface of the world as they form complex networks across landscapes. Overall, an estimated 2×10^{15} g C per year are transported, transformed, or stored by streams and rivers on earth, and 3.2×10^{14} g C are respired as CO_2, an important greenhouse gas [31]. While an estimated 33% of carbon emitted from streams is predicted to pass through a viral shunt [10], the specific roles of viruses in lotic systems have yet to be described. Therefore, an important goal of this study is to characterize viral control on ecological processes of stream ecosystems [10]. Microbial assemblages attached to hard substrata of riverbeds, i.e. biofilms, are the foundation of the riverine food web, especially in headwaters [31,32]. Consequently, composition and metabolic activity of biofilms have a major influence on

* Corresponding author. 2127 Integrated Science Center, Williamsburg, VA 23186, USA.
E-mail addresses: jkan@stroudcenter.org (J. Kan), mpeipoch@stroudcenter.org (M. Peipoch), kewilliamson@wm.edu (K. Williamson).

https://doi.org/10.1016/j.bioflm.2019.100016
Received 15 September 2019; Received in revised form 6 November 2019; Accepted 29 November 2019
Available online 6 December 2019

the biogeochemistry and productivity of lotic systems. For instance, stream biofilms are intimately linked to carbon flux globally and emit an outsized amount of carbon into the atmosphere, compared to the global surface area of streams, through the degradation of organic matter [31,33].

Much of our current knowledge regarding biofilms comes from lab-scale studies using single-species biofilms. Such approaches have been highly valuable in developing conceptual models to understand biofilm formation and development [34], biofilm interactions with the surrounding environment [35], and biofilm interactions with other microbes [36]. However, streams have multispecies and frequently, polymicrobial biofilms which are the greatest reservoir of microbial diversity in lotic systems [31,37,38]. Almost nothing is known regarding the potential roles of viruses in these communities. What little information is available comes from laboratory-scale studies using single species biofilms [39]. Furthermore, the potential importance of lysogenic replication is not well understood in stream biofilms. It could be predicted that the matrix that covers biofilm communities provides physical protection from infection by extracellular phages, and therefore selects for lysogenic replication by phages within biofilm communities.

The main goals of this work were to: 1) determine whether viruses (detectable as extracellular particles) are consistent members of natural mixed biofilm communities; 2) determine whether temperate phage (detectable as inducible prophages) are consistent members of multi-species bacterial biofilms collected from streams; and 3) to determine whether community profiling approaches like RAPD-PCR can be adapted to characterize and compare biofilm virus communities. Our hypotheses were: 1) virus-like particles would be detectable in the biofilm matrix and be consistent members of the polymicrobial community; and 2) temperate phages are prevalent in bacterial biofilms of streams since the spatial structure of biofilms presents a physical barrier to extracellular attack and prophage could be maintained within lysogenic cells in the active layer community.

Materials and methods

Field sites and sample collection

Crim Dell Creek

Biofilm growth was cultivated on stones deployed in the stream bed of Crim Dell Creek, a stream that drains the Crim Dell pond on the campus of the College of William and Mary, Williamsburg, VA, USA. Cement 7″ by 7” (17.8 × 17.8 cm) steppers were deployed on 02/01/2017 in three different reaches of the stream: Crim Dell Pond (CDP, 37°16′14.4″N, 76°42′52.4″W; Fig. 1) in the immediate outflow from the pond, Crim Dell upper reach (CDU, 37°16′15.5″N, 76°42′58.5″W; Fig. 1), and Crim Dell lower reach (CDL, 37°16′12.8″N, 76°43′03.8″W; Fig. 1). Three replicate stones were completely submerged at each location in a row across the width of the stream bed. One of the three replicate stones was collected from each site at 51, 70, and 105 days post-deployment, and biofilm material was harvested in the lab. Biofilm extraction is described below.

White Clay Creek

Natural biofilm samples were collected from the streambed of White Clay Creek (WCC) in Avondale, PA (39°51′35.1″N, 75°46′58.2″W). Samples of sediment-associated streambed biofilms were gathered from WCC adjacent to Stroud Water Research Center (39°51′33.5″N 75°47′01.6″W) on a monthly schedule from August 2016 through February 2017. Samples were generally collected on the first Wednesday of each month, but sampling times were adjusted to avoid large scale disturbances such as storm events. At each sampling site triplicate samples were gathered from the left, center, and right streamlines. These triplicate samples were pooled on site, yielding one aggregate sample each month. During sediment collection, a 40 mm diameter plastic ring was used to remove a small circular plug of streambed. The top layer of this plug, corresponding to the uppermost layer of streambed sediments was scraped using a flat blade and stored in a sterile Whirl-pak bag (Nasco, Pacifica Palisades, CA) for transport to the lab. Sediments and associated biofilm were then transferred into sterile 2 ml tubes and frozen at -80 °C until use.

Experimental flumes

Biofilm samples were grown in indoor experimental flumes (6.1 m long x 0.43 m wide x 0.2 m deep; average water height 0.1 m) at Stroud Water Research Center, Avondale, PA. The water used in flume experiments originated from WCC, which is directly adjacent to the research center, and supplied to flumes in a once-through design. Flumes were switched to recirculation July 2–3, 2018 and July 21–23, 2018 due to storm events that would have changed the nutrient concentrations and sediment load of the intake water relative to base flow conditions. Nutrient concentrations for WCC typically range from 3 to 4 mg NO_3–N l^{-1} and 10–60 g PO_4–P l^{-1} [40]. The middle 5 m of the length of all flumes were packed with autoclaved rocks (median diameter 5 cm) obtained from WCC as substrate for biofilm growth. Average water temperature in the flumes was 20.8±1.5 °C for the duration of the experiments. Biofilms in the experimental flumes were cultivated for approximately 5 weeks, from June 25, 2018 to August 3, 2018. Four flumes were established with

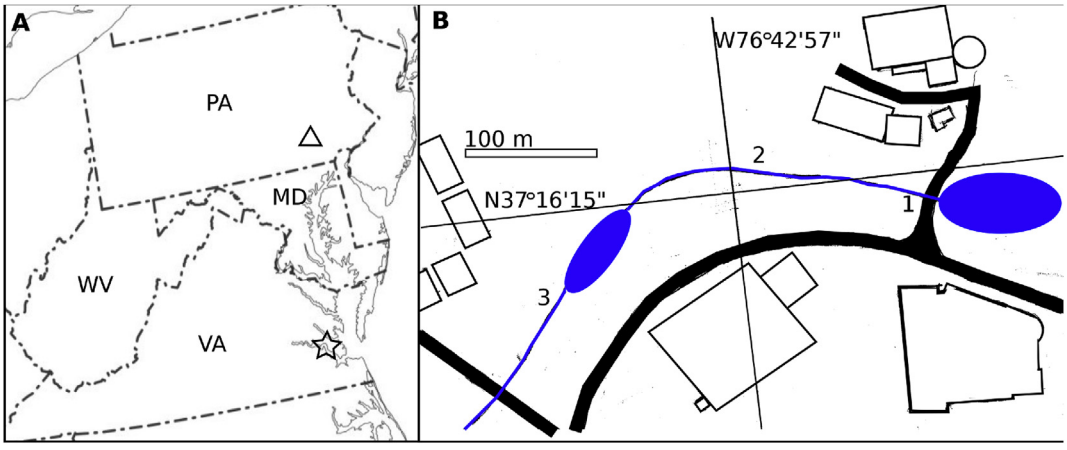

Fig. 1. A) Sampling locations; star = College of William & Mary, Williamsburg, VA; triangle = Stroud Water Research Center, Avondale, PA. B) Field sites where natural biofilm samples were collected along the Crim Dell Creek on the campus of the College of William and Mary. 1, Crim Dell Pond; 2, Crim Dell Upper reach; 3, Crim Dell Lower reach.(Figure should appear in color). (For interpretation of the references to color in this figure legend, the reader is referred to the Web version of this article.)

the following treatments and conditions:

Flume 1

High flow storm treatment. Water was supplied at a continuous base flow rate of approximately 0.2 m s^{-1} pre-storm. The flow rate was then adjusted on July 12 (after approximately 2.5 weeks of biofilm growth) to mimic a 24-h high velocity storm (0.4 m s^{-1}) with sediment added (410 nephelometric turbidity units, NTU). The flow rate was adjusted back to pre-storm conditions after the 24-h pulse (Fig. 2).

Flume 2

Recolonized new rocks. No water was supplied to this flume until July 12, and the first water flow simulated a 48-h storm pulse (0.3 m s-1) with sediment added (479 NTU). After the storm pulse, the flow rate was adjusted to the base flow rate of approximately 0.2 m s^{-1} for the remainder of the observation period (Fig. 2).

Flume 3

Low flow storm treatment. Water was supplied at a continuous base flow rate of approx. 0.2 m s^{-1} pre-storm. The flow rate was then adjusted on July 12 (after approximately 2 weeks of biofilm growth) to mimic a 48-h low velocity storm (0.3 m s^{-1}) with sediment added (417 NTU). The flow rate was adjusted back to pre-storm conditions after the 48-h pulse (Fig. 2).

Flume 4

Control/Continuous flow. Water was supplied at a continuous base flow rate of approximately 0.2 m s^{-1} over the five-week observation period (Fig. 2).

Extraction of bacteria and virus particles from biofilm samples

Field sites

Extraction procedures were developed based on [41]. Biofilm material was scraped off of the collected stone (Crim Dell Creek samples) or top layer of streambed sediments (White Clay Creek samples) for each site using a razor blade and placed in separate 15 mL polypropylene tubes, one tube per site. The pooled biofilm scrapings from a single stone/site were homogenized by manual mixing with a sterile spatula and then portioned out into four 0.1 g replicates in pre-weighed 1.5 mL microcentrifuge tubes. De-ionized water (800 μL) and 80 μL of 0.1 mM EDTA were added to each tube and tubes were vortexed for 30 s before incubating at room temperature (ca. 22 °C) for 15 min in the dark. Each tube was sonicated for five rounds of 10 s with 10 s of rest in between, using a Branson 3 mm ultra-high intensity sonifier probe (Thomas Scientific, Swedesboro, NJ) with a maximum output of 494 Amps set at 10% output. Afterwards, each replicate was incubated with 1 μL of cyanase, a high-efficiency nuclease that degrades both DNA and RNA (RiboSolutions, Inc., Cedar Creek, TX), and 1 μL $MnSO_4$ (1 M) at 37 °C for 30 min.

Two of the four replicates were designated for bacterial extraction. For these tubes, approximately 1 mL of sonicated biofilm material was layered over 200 μL Nycodenz (1.3 g/mL) (Accurate Chemical, Westbury, NY), in a sterile 1.5 mL microcentrifuge tube. Tubes were centrifuged in an Eppendorf 5402 Centrifuge (Eppendorf, Hamburg, Germany) for 15 min at 14,000 rpm and 4 °C. After centrifugation, the supernatant was carefully pipetted into a sterile 1.5 mL microcentrifuge tube and stored on ice until used for slide preparation within 1 h.

The remaining two replicates were designated for virus particle extraction. Tubes were centrifuged in an Eppendorf Centrifuge 5402 (Eppendorf, Hamburg, Germany) for 15 min at 14,000 rpm and 4 °C. The supernatant was carefully decanted into a barrel of a sterile 3 mL syringe with a 0.22 μm filter (Millipore, Billerica, MA) attached. The supernatant was filtered into a sterile 1.5 mL microcentrifuge tube and stored on ice until used for slide preparation within 1 h.

Experimental flumes – microbial abundance

Frozen samples were thawed on ice. Phage buffer (150 mM NaCl, 40 mM Tris-Cl, pH 7.4, 10 mM $MgSO_4$, 1 mM $CaCl_2$) was added to each 2 mL microcentrifuge tube until the cotton swab tip was completely covered. Tubes were vortexed for 1 min and the cotton swab head was removed using ethanol-sterilized forceps. Tubes were then centrifuged at 8000×*g* for 15 min and at 4 °C to pellet the biofilm material. The supernatant was decanted, and the mass of pelleted biofilm material was estimated based on the average tare mass of ten 2 mL microcentrifuge tubes. After the supernatant was removed, bacterial cells and virus particles were extracted simultaneously by sonicating samples and centrifuging on Nycodenz cushions as described above.

Experimental flumes – prophage induction

For biofilms grown in experimental flumes, three rocks were selected from each flume (beginning, middle, and end of each flume) and biofilm material was scraped off with a razor blade. The harvested biofilm material was pooled in sterile 15 ml tubes, one tube per flume, and homogenized by manual mixing with a sterile spatula. Aliquots (0.1 g) of

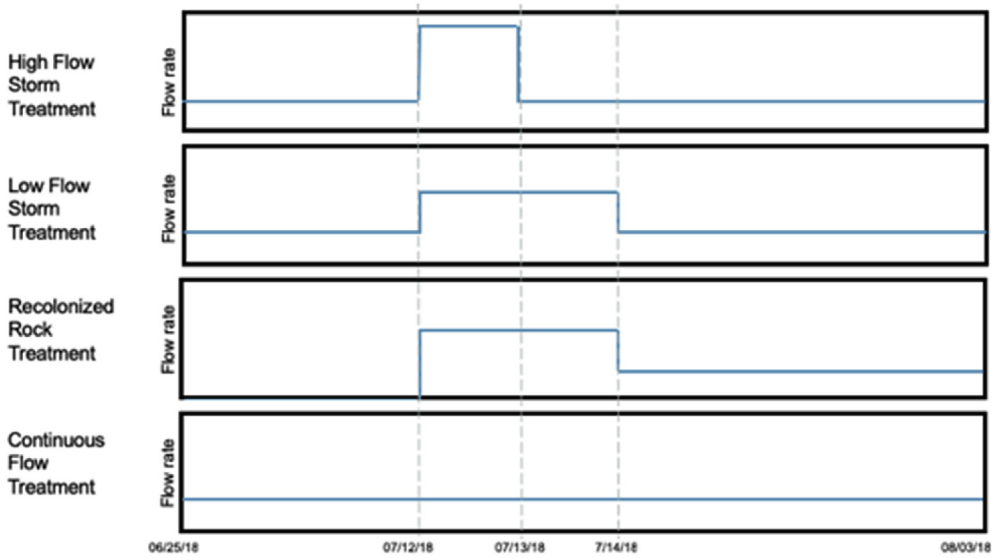

Fig. 2. Flow rates and treatment conditions of the four experimental flumes (High-Flow Storm Treatment, Low-Flow Storm Treatment, Recolonized Rock Treatment, and Continuous Flow Treatment) built at Stroud Water Research Center with water diverted from White Clay Creek.

homogenized biofilm were weighed into 6 replicate 1.5 mL microcentrifuge tubes, which were processed simultaneously and pooled later. Deionized water (800 μL) and 80 μL of 1 mM EDTA were added to each tube, and tubes were processed as described above for bacterial extractions from Field Site samples.

Prophage induction

Field sites

Aliquots (~100 μL) of bacterial extracts from each site were transferred into sterile microcentrifuge tubes and reserved for future epifluorescence microscopy slides. The remaining bacterial extract in each replicate tube was split into duplicate control and treatment tubes, each tube receiving ~500 μl of bacterial extract. Mitomycin C (Fisher, Pittsburgh, PA) was added to each treatment tube at a final concentration of 0.5 μg mL^{-1} and an equivalent volume of deionized water was added to each control tube. Tubes were secured to a rocking table (LabNet, Edison, NJ) set at 50 RPM and incubated in the dark for 24 h at room temperature (ca. 22 °C). At the end of the incubation period, all tubes were frozen with liquid nitrogen and stored at -80 °C until analysis by epifluorescence microscopy.

Experimental flumes

Inductions were carried out as described for Field Sites, above, except that all experiments involved triplicate control and treatments, and 1 ml of biofilm bacterial extract was used for each replicate.

Epifluorescence microscopy

Field sites

Bacteria and virus extracts were prepared separately (see extraction protocol) and therefore were enumerated separately. For viral enumeration, 100 μl aliquots of the biofilm viral extracts were suspended in 900 μL of sterile deionized water in a labeled microcentrifuge tube. After mixing the samples by vortexing, the suspension was filtered onto Whatman 13 mm 0.02 μm pore Anodisc filters (Whatman, Maidstone, England) in individual Swinnex plastic filter holders (Millipore, Billerica, MA) using a Welch 60 Hz vacuum pump (Welch, Mt. Prospect, IL). Filters were stained with 100 μL 2.5 X (final concentration) SYBR gold (Invitrogen, Carlsbad, CA) for 15 min in the dark. The stain solution was then drawn through the filters under vacuum, the filters removed from the Swinnex holders using forceps, and filters were allowed to air dry on a Kim-wipe in the dark for approx. 15 min. Dried filters were mounted on glass microscope slides 5 μL of antifade (0.1 g p-phenylenediamine in 9 mL glycerol). A glass coverslip was then placed on top of each filter with another 5 μL of antifade between the coverslip and filter. Slides were stored in the dark at -20 °C until examined using epifluorescence microscopy.

For bacterial enumeration, 100 μl aliquots of the biofilm bacterial extracts were suspended in 900 μL of sterile deionized water in a labeled microcentrifuge tube. After mixing the samples by vortexing, the suspension was filtered onto black Whatman 25 mm Isopore filters with a 0.2 μm pore size (Whatman, Maidstone, England) using a filter manifold (Millipore, Billerica, MA). Isopore filters were placed over a glass fiber support filters (GF/F, Pall, New York, NY). Samples were vacuumed through the filter stack, stained with 2.5 X SYBR Gold, air dried, mounted on glass microscope slides and stored as previously described.

Experimental flumes

Viruses and bacteria were not extracted separately, thus, both bacteria and virus particles were enumerated using a single extract for each sample. The protocol for slide preparation was identical to the virus protocol outlined above, except that extracts were not filtered through 0.22 μm. Aliquots of 100 μL or 250 μL of extract diluted to 1 mL with deionized water depending on density of VLPs and cells observed under fluorescence microscopy.

Epifluorescence microscopy

Slides were imaged using an Olympus BX51 microscope (Olympus, Center Valley, PA) fitted with a 100x/1.30 oil lens, Olympus U-RFL-T mercury lamp (Olympus, Center Valley, PA) and FITC excitation filter. A minimum of 10 images per Anodisc filter (100 bacterium-sized objects, 200 virus-sized objects) were captured using a Hamamatsu C8484 digital camera (Hamamatsu Corporation, Bridgewood, NJ). Image analysis was conducted using MetaMorph (MetaMorph, Nashville, TN), wherein bacterial cells and virus particles were discriminated and counted based on calibrated dimensions as previously described [42].

Transmission electron microscopy

Triplicate biofilm extracts from the continuous flow flume were pooled and suspended in TMG buffer (0.5 M Tris pH 8.0, 150 mM $MgCl_2$, 10% glycerol). Virus suspensions were pelleted by ultracentrifugation at 150,000×*g* in an SW41–Ti rotor (Beckman Coulter, Brea, CA) for 90 min at 10 °C. Viral pellets were resuspended in 0.1 M ammonium acetate and pelleted again under the same ultracentrifuge conditions. Viral pellets were resuspended in 500 μl of TMG buffer. Ten microliters of virus resuspension were applied to formvar-coated copper TEM grids (400 mesh, Ted Pella, Redding, PA) and grids were incubated at room temperature for 5 min. Grids were stained with 2% uranyl acetate (aq.) for 1 min and rinsed twice with deionized water for 1 min each rinse. Grids were air dried for 24 h before examination in a Philips CM 10 TEM (Philips, Amsterdam, Netherlands) at 80 kV. Micrographs were obtained using an AMT XR80S–B 8 MP camera (AMT, Woburn, MA).

Comparison of biofilm viral communities using randomly amplified polymorphic DNA – polymerase chain reaction (RAPD-PCR)

Sample collection

Natural stones (i.e., pre-existing in the steam bed and not deployed) were collected at CDP on March 29, 2018. Biofilm material was collected as previously described and aliquoted into eight 0.1 g replicates. Each replicate was extracted and treated with cyanase as previously described. All replicates were then flash frozen with liquid nitrogen after extraction was completed and stored at -80 °C until use.

Concentration of biofilm viral extract

Of the eight replicate biofilm extractions, two replicates were pooled into one polyallomer ultracentrifuge tube, and two additional replicates were pooled into another tube (Beckman-Coulter, Pasadena, CA). Tubes were spun in an Optima XPN-90 ultracentrifuge (Beckman-Coulter, Pasadena, CA) for 1.5 h at 178,000×*g* and 4 °C. Virus pellets were resuspended in 100 μL of phage buffer and transferred to a sterile 1.5 ml microcentrifuge tube.

Preparation of control DNA

Control extracellular DNA was prepared from T4 phage by amplifying the g23 gene according to previously published PCR conditions [43]. Five replicate PCRs were pooled and purified using a Qiagen QIAquick PCR Purification Kit (Qiagen, Germantown, MD) according to the manufacturer's instructions. The concentration of the g23 DNA was 67.5 ng μL^{-1}.

Eliminating extracellular DNA from biofilm viral concentrates

The remaining four replicates of CDP biofilm virus extract were concentrated as described above, diluted 1:1 with phage buffer and each sample was spiked with 67.5 ng of g23 DNA. Aliquots (5 μL) of the spiked samples were transferred into sterile 0.5 mL microcentrifuge tubes to serve as the initial time point and then stored at 4 °C until PCR amplification. The remaining samples were subjected to three repeated rounds of cyanase treatment to test removal extracellular DNA. For each round of cyanase treatment, 1 μL of cyanase and 1 μL of $MnSO_4$ (1 M) were added to each spiked sample and tubes were incubated at 37 °C for 30 min. After

incubation, 5 μL aliquots of each sample were transferred into sterile 0.5 mL microcentrifuge tubes and stored at 4 °C until PCR amplification. The remaining spiked sample was extracted with 200 μL of chloroform and centrifuged in an Eppendorf Centrifuge 5402 (Eppendorf, Hamburg, Germany) at 3000 rpm and 4 °C for 30 min to remove the nuclease, as previously described [44]. The aqueous layer was transferred to a new tube and cyanase treatment (and chloroform extraction) was repeated for three more rounds. After each round of treatment, 5 μL aliquots of the samples were collected and stored at 4 °C. All aliquots, including the initial, untreated spiked samples, were used as templates in PCR amplification using g23-specific primers as previously described [45].

Analysis of reproducibility

Quadruplicate biofilm bacterial extracts from CDP were induced with Mitomycin C as previously described. After induction, each sample was centrifuged in an Eppendorf Centrifuge 5402 (Eppendorf, Hamburg, Germany) at 14,000 rpm and 4 °C for 15 min, supernatants were filtered through 0.22 μm and the filtrate collected into sterile 1.5 ml microcentrifuge tubes. Replicates were pooled to create two composite samples in two separate 1.5 ml tubes. Each composite sample was treated with 1 μL cyanase and 1 μL of $MnSO_4$ (1 M) at 37 °C for 30 min.

RAPD-PCR was performed using the CRA-22 primer (5′-CCG CAG CCA A- 3′) as previously described [46]. Triplicate reactions (technical replicates) were run for each pooled sample in order to verify the reproducibility of results. A second round of RAPD-PCR was performed for each replicate by using 1 μL of products from the first round as template in another round of amplification. Both rounds of RAPD-PCR included a positive control (1 μL of DNA known to produces bands) and a negative control (1 μL of DEPC H_2O) to confirm proper amplification and no contamination.

RAPD-PCR products were resolved using a 2% high-resolution agarose gel [MetaPhor high-resolution RAPD-PCR agarose (Lonza, Alpharetta, GA)] prepared using 1x TBE buffer. Invitrogen TrackIt 100 bp DNA ladder (Invitrogen, Carlsbad, CA) was used as a size standard. Gels were run for 2 h at 90 V and 500 mA using a LabNet 300 V gel electrophoresis power supply (LabNet, Edison, NJ). The gel was stained in 1X SYBR gold (Invitrogen, Carlsbad, CA) made up in 0.5 X TBE for 1 h prior to imaging. Band pattern analysis was performed using ImageQuant TL v. 7.0 (GE Healthcare Life Sciences, Chicago, IL). Band sizes were sorted into 10-bp bins using the molecular weight markers as references, and each specific bin was interpreted as a viral operational taxonomic unit or OTU [42]. Using this binning approach, a binary matrix of viral OTU presence/absence was created and used in subsequent analyses.

RAPD-PCR analysis of experimental flumes

The experimental flume biofilm extracts from the continuous flow flume collected on June 25, 2018, July 10, 2018, July 23, 2018, and August 3, 2018 were used for RAPD-PCR analysis of change in biofilm viral community composition over approximately two months. Extracts were thawed on ice and centrifuged at 14,000 rpm and 4 °C for 15 min. The supernatant was carefully poured off into a sterile 3 mL syringe with a 0.22 μm filter (Millipore, Billerica, MA) attached to remove the bacterial cells. The supernatant was filtered into a new microcentrifuge tube for RAPD-PCR amplification as described previously. Three replicate reactions were run for each sample, and RAPD-PCR was performed in two consecutive rounds to reach adequate concentration of DNA to visualize banding patterns. Gels were imaged and a binary matrix generated as previously described.

Calculations

The number of viruses or bacteria per milligram of biofilm was calculated by first taking the average number of cells or virus particles over ten pictures per sample. This average was then used to calculate the number of virus or bacterial particles over the whole Anodisc slide as previously described [42].

The prophage induced (P_i) was calculated by subtracting the viral direct count (VDC) in the control from the VDC in the treatment:

$$P_i = VDC_{Treatment} - VDC_{Control}$$

Induction assays in which VDC of mitomycin C-treated samples was significantly (95% CI) higher than paired, untreated controls were scored as positive for induction [47]. The virus to bacterium ratio (VBR) was calculated for each sample with the following equation [24]:

$$VBR = VDC\ mg^{-1} / BDC\ mg^{-1}$$

The inducible fraction (IF) was calculated using three different burst sizes: $B_z = 50$, $B_z = 30$, or the mortality method. As described previously, IF for each sample is reported as a percentage of the bacterial community [24]:

$$IF\ (\%) = (Pi / Bz) / BDC_{Control}\ X \qquad 100$$

Statistical and other analyses

Abundance

Values for both abundance graphs and inductions were determined using epifluorescence microscopy direct counts. ANOVA was used to test for differences in bacterial and viral abundances across sites and over time, using Prism 8 (GraphPad, San Diego, CA).

Inductions

Paired t-tests (95% CI) were performed using Prism 8 (GraphPad, San Diego, CA) and used to test whether viral direct counts were significantly higher in mitomycin C-treated samples relative to untreated controls. Statistically higher VDC in treatment samples were scored positive for induction.

RAPD-PCR band analysis

Banding patterns from RAPD-PCR were converted into a binary matrix that was analyzed using non-metric multidimensional scaling (NMDS) and cluster dendrograms created in PAST [48]. Ordination analysis was used to compare the similarity and dissimilarly of the banding patterns across samples [42].

Results

Microbial abundance

Field sites: Crim Dell Creek

At each location, the bacterial direct count (BDC) per mg biofilm increased over time, with the largest increase occurring between 04/12/17 and 05/01/17 (Fig. 3A). At the CDL location, there was a slight decrease from 03/24/17 to 04/12/17 (Fig. 3A). With the exception of the March 2017 sample, the BDC in biofilms obtained from CDU were consistently higher than biofilms obtained from the other two sites. However, there was no significant difference between locations (one-way ANOVA; $p = 0.3066$). Likewise, no significant differences were observed in BDC across time, irrespective of location (one-way ANOVA; $p = 0.3319$, $r = 0.4463$). Given this lack of clear trend or pattern in growth, a longer-term analysis of BDC encompassing more than 3 months of growth, or more frequent sampling intervals than once a month, may help illuminate relationships over time and space.

Comparison of viral direct counts (VDC) from biofilm extracts over time did not show a consistent trend, due in part to missing data points for CDU 03/24/17 and CDU 04/12/17. These samples were collected, but due to the loss of the slides for epifluorescence microscopy, microbial abundance could not be determined. Generally, VDC was highest on 03/24/17 and viral abundance decreased for both CDP and CDL from 03/24/

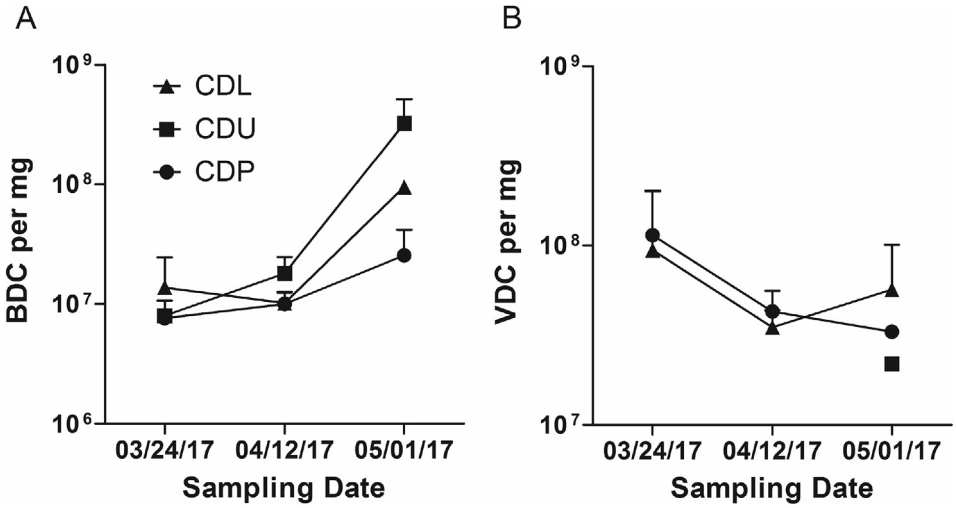

Fig. 3. A) The bacterial direct count (BDC) mg^{-1} biofilm at each sampling location for the natural biofilms over time. Error bars represent range (N = 2). B) The viral direct count (VDC) at each sampling location for the natural biofilms over time. Error bars represent range (N = 2).

17 to 04/12/17 (Fig. 3B). However, CDP and CDL diverged from 04/12/17 to 05/01/17, with a decrease at CDP and an increase at CDL. The trend over time cannot be analyzed for CDU (Fig. 3B). While the overall trend for viruses appeared to be decreasing over time during the sampling interval, virus particles were observed in the biofilm communities at consistently high numbers, 10^7 mg^{-1} or greater.

Field sites: White Clay Creek

Bacterial abundance generally increased from August through January, but rather sharp drops in abundance were observed for both October and February (Fig. 4A). Total abundances ranged from $5.53 \times 10^5 \pm 3.72 \times 10^5$ cells mg^{-1} in October to $1.96 \times 10^6 \pm 3.54 \times 10^5$ cells mg^{-1} in January (Fig. 4A).

Trends in viral abundance in the WCC biofilm samples did not appear to mirror the bacterial abundance trends. Viral abundance peaked in December (Fig. 4B), while bacterial abundance peaked in January, one month after the peak in viral abundance (Fig. 4A). Viral abundance before and after the observed December peak remained relatively constant and VDC ranged from $1.17 \times 10^6 \pm 8.37 \times 10^5$ in October to $6.83 \times 10^6 \pm 2.18 \times 10^6$ in December (Fig. 4B). Interestingly, the drop in BDC observed in October was not paralleled by a drop in VDC in the same sample, which suggests a decoupling between viral and bacterial dynamics in the biofilm.

The virus to bacteria ratio (VBR) was determined for this time series, as a means to assess potential linkages between bacterial and viral dynamics. The ratios fluctuated from month to month, with the highest ratio coinciding with the maximum BDC in January and the lowest ratio coinciding with the maximum VDC in December (Fig. 4C).

Experimental flumes

The high-flow and low-flow flumes exhibited similar trends in bacterial abundance over time (Fig. 5A). The continuous flow flume had a large spike in BDC on 07/03/18 and all three flumes exhibited an increased in BDC on 08/03/18 (Fig. 5A). The high-flow and low-flow flumes exhibited fairly similar trends in viral abundance over time (Fig. 5B). In the continuous flow flume, both BDC and VDC in the biofilm peaked on 07/03/18, and the biofilm communities of all three flumes had increased in both bacterial and viral abundance by 08/03/18, relative to initial observations (Fig. 5B). Similarities in bacterial and viral abundance across the three different flow regimes suggests that the simulated storm flows did not strongly affect total microbial abundances in biofilms. Alternatively, perhaps the storm flow rates used in these

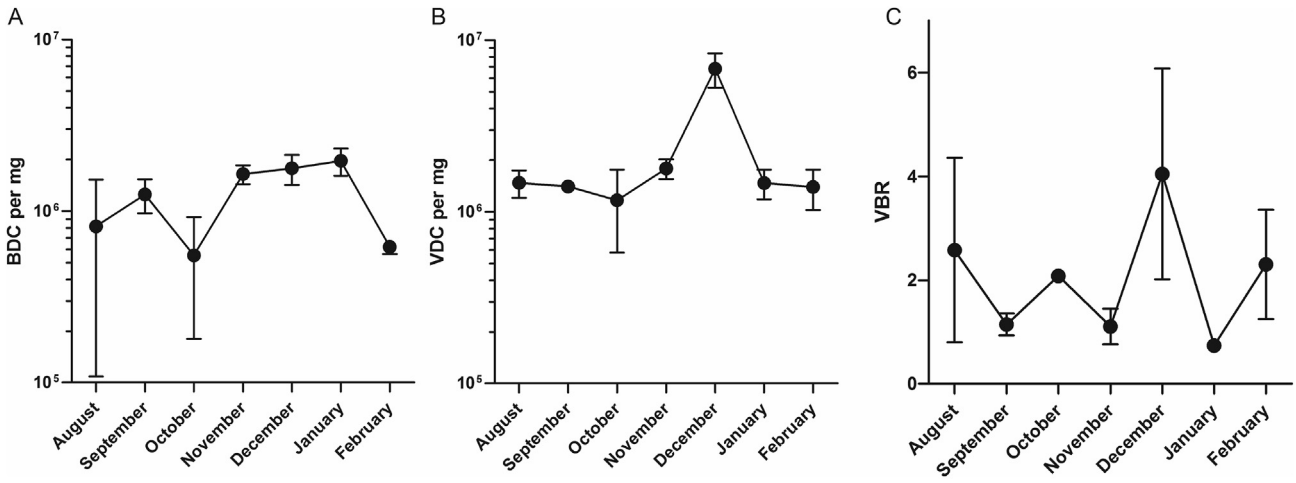

Fig. 4. A) The bacterial direct count (BDC) mg^{-1} biofilm for the White Clay Creek biofilm samples over the months of August to February. Error bars represent range (N = 2). B) The viral direct count (VDC) for White Clay Creek flume biofilms samples over the months of August to February. Error bars represent range (N = 2). C) The ratio of bacteria to viruses for the White Clay Creek biofilms samples over the months of August to February. Error bars represent range (N = 2).

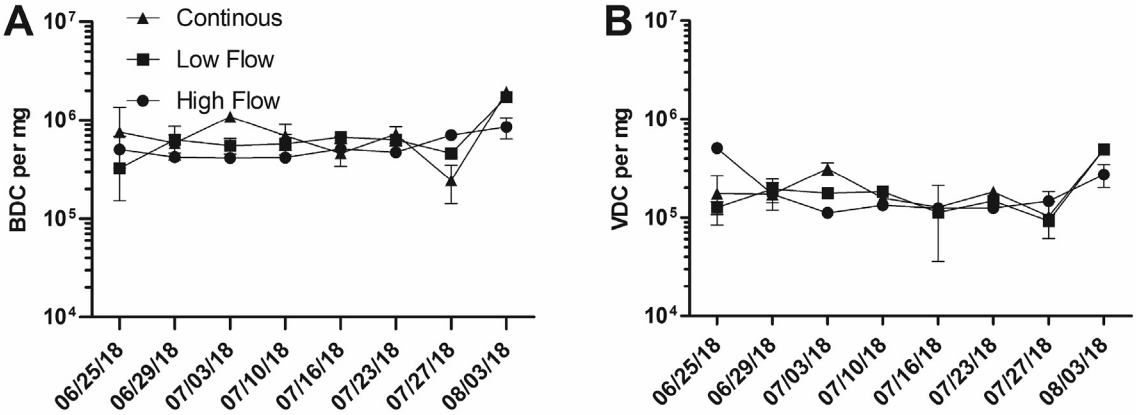

Fig. 5. A) The bacterial direct count (BDC) mg^{-1} biofilm for the experimental flume biofilms samples from 06/29/18-08/03/18. Error bars represent range (N = 2). B) The viral direct count (VDC) for the experimental flume biofilms samples from 06/29/18-08/03/18. Error bars represent range (N = 2).

experiments were not high enough to cause significant differences in biofilm microbial abundances.

TEM analysis of experimental flume biofilm viruses

Transmission electron microscopy was used to analyze biofilm extracts for visual evidence of phage particles within the biofilm community, revealing a diversity of viral morphologies (Fig. 6). Taken together, both viral abundance data from epifluorescence microscopy and the electron micrographs suggest that viruses are present and active within natural streams and laboratory-grown polymicrobial biofilm samples.

Induction assays

Field sites

Bacterial cells extracted from Crim Dell Creek biofilms were subjected to induction assays to test for the presence and prevalence of bacterial lysogens harboring prophages (Table 1). Only three samples showed no evidence of prophage induction: CDL 03/24/17, CDU 04/12/17, and CDU 05/01/17 (Table 1). However, six out of nine (66.7%) of the field site biofilms did show evidence of prophage induction; i.e., statistically significant increase in viral particles in the mitomycin C-treated samples relative to untreated controls (Table 1). Prophage induction was significant ($p = 0.0108$), with the average number of prophages induced across

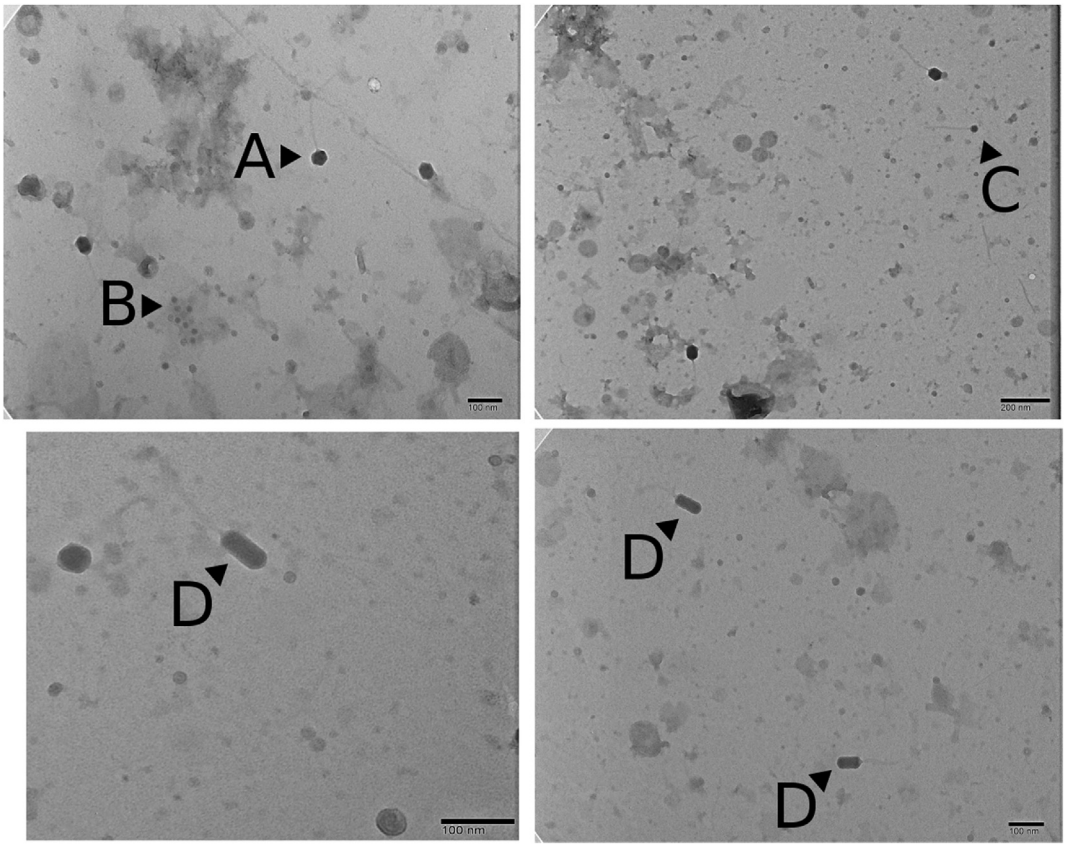

Fig. 6. Example electron micrographs of biofilm viruses. A) virus particle exhibiting *Siphoviridae* morphology, B) cluster of icosahedral virus particles, C) *Siphoviridae* with small capsid, D) *Siphoviridae* with prolate capsids.

Table 1
Induction assay results for Crim Dell Creek Biofilm samples VDC mg^{-1}.

Sample	Treatment	Control	% Change
CDP 03/24/17	$1.46 \times 10^7 \pm 2.24 \times 10^5$	$1.19 \times 10^7 \pm 3.16 \times 10^5$	22.68
CDU 03/24/17	$3.49 \times 10^6 \pm 1.37 \times 10^6$	$2.57 \times 10^6 \pm 3.47 \times 10^5$	35.79
CDL 03/24/17	$3.04 \times 10^6 \pm 1.04 \times 10^6$	$4.35 \times 10^6 \pm 2.14 \times 10^5$	-30.11
CDP 04/12/17	$1.11 \times 10^7 \pm 3.27 \times 10^6$	$6.79 \times 10^6 \pm 1.19 \times 10^6$	63.47
CDU 04/12/17	$4.24 \times 10^6 \pm 5.17 \times 10^5$	$9.48 \times 10^6 \pm 6.44 \times 10^5$	-55.27
CDL 04/12/17	$6.11 \times 10^6 \pm 1.00 \times 10^6$	$2.51 \times 10^6 \pm 2.40 \times 10^5$	143.42
CDP 05/01/17	$1.00 \times 10^7 \pm 3.34 \times 10^6$	4.43×10^6	125.73
CDU 05/01/17	9.01×10^6	$1.72 \times 10^7 \pm 1.86 \times 10^5$	-47.61
CDL 05/01/17	$9.06 \times 10^6 \pm 1.11 \times 10^6$	$8.12 \times 10^6 \pm 2.21 \times 10^6$	11.57

Viral Direct Count (VDC) per milligram of biofilm obtained from epifluorescence microscopy. Results are represented as averages between replicates ± range (N = 2).

Table 2
Calculations of the Inducible Fraction for Crim Dell Creek induction assays Inducible Fraction Calculation.

Sample	Prophage induced mg^{-1}	$B_Z = 50$	$B_Z = 30$	Mortality Method	Induced B_Z
CDP 03/24/17	$1.39 \times 10^6 \pm 3.38 \times 10^6$	0.064 ± 0.16	0.107 ± 0.27	0.472 ± 1.65	6.79 ± 16.56
CDU 03/24/17	$4.61 \times 10^5 \pm 1.02 \times 10^6$	0.021 ± 0.049	0.035 ± 0.081	0.0249 ± 0.079	42.81 ± 95.75
CDP 04/12/17	$2.14 \times 10^6 \pm 2.08 \times 10^6$	0.099 ± 0.11	0.165 ± 0.19	-0.451 ± 0.78	-10.97 ± 14.23
CDL 04/12/17	$1.80 \times 10^6 \pm 1.24 \times 10^6$	0.083 ± 0.078	0.139 ± 0.13	-0.600 ± 2.75	-6.92 ± 31.00
CDP 05/01/17	2.93×10^6	0.135 ± 0.086	0.226 ± 0.14	0.513 ± 0.51	13.20 ± 10.14
CDL 05/01/17	$4.72 \times 10^5 \pm 1.10 \times 10^6$	0.022 ± 0.053	0.036 ± 0.088	0.0526 ± 0.18	20.73 ± 49.04

B_z = bacterial burst size; VDC = viral direct count; BDC = bacterial direct count. Results are represented as averages between replicates ± range (N = 2).

Table 3
Induction assay results for experimental flume biofilms VDC mg^{-1}.

Flume Condition	Treatment	Control	% Change
Initial	$1.14 \times 10^6 \pm 3.30 \times 10^5$	$4.63 \times 10^5 \pm 1.83 \times 10^4$	147.50
Continuous	$4.83 \times 10^6 \pm 2.03 \times 10^6$	$1.43 \times 10^6 \pm 5.15 \times 10^5$	238.55
High Flow	$1.98 \times 10^6 \pm 5.39 \times 10^5$	$8.77 \times 10^5 \pm 3.62 \times 10^5$	125.52
Low Flow	$6.26 \times 10^5 \pm 8.82 \times 10^4$	$7.02 \times 10^5 \pm 5.05 \times 10^5$	-10.80
New Rocks	$1.04 \times 10^6 \pm 4.79 \times 10^5$	$1.38 \times 10^6 \pm 1.84 \times 10^5$	-24.51

Viral Direct Count (VDC) per milligram of biofilm obtained from epifluorescence microscopy. Results are represented as averages between replicates ± SD (N = 3).

all sample times and locations $1.51 \times 10^6 \pm 9.29 \times 10^5$ virus particles mg^{-1} biofilm. This average remained relatively stable across samples, indicating that it may be independent of sample timing or sample location (Fig. 7A). Therefore, prophages may be stably maintained within the biofilm community.

Grouping the prophage induction results by sampling location did not reveal any relationships by site or by date (Fig. 7B). It is likely that the number of samples tested was not large enough or the sampling time scale was too coarse to detect any broader patterns. Inducible fraction calculations were carried out for all of the biofilm samples showing positive induction. The average inducible fraction across all Crim Dell Creek biofilm samples was 0.0708 ± 0.0448 using an estimated burst size of 50; 0.118 ± 0.0746 using an estimated burst size of 30; and 0.00181 ± 0.459 using the mortality method (Table 2). These percentages are very small compared to total bacterial abundance in the biofilm, comprising less than 1% of the biofilm community irrespective of the calculation method. The average induced burst size (mortality method) was 10.94 ± 19.66 and two samples (CDP 04/12/17 and CDL 04/12/17), produced negative ΔVDC/ΔBDC ratios, prohibiting the calculation of burst size (Table 2).

Experimental flumes

Significant differences were observed in VDC between control and induced samples across all flumes (p = 0.036; Table 3, Fig. 8A). The initial 07/03/18 sample, continuous flow flume, and high-flow flume showed significant evidence of prophage induction (p = 0.0125; Fig. 8B). In particular, the continuous flow flume had the highest level of prophage induction (Fig. 8B). The prophage abundances observed in both laboratory-grown biofilms and natural biofilms obtained from field sites, as well as biofilms at different stages of growth and development, support the hypothesis that temperate phages are consistent members of biofilm communities and play a role in the dynamics of stream biofilms.

The grand average inducible fraction (expressed as a percentage of total extracted cells) across all experimental flume biofilms was 0.110 ± 0.094 using an assumed burst size of 50; 0.184 ± 0.156 using an assumed burst size of 30; and 40.9 ± 17.6 using the mortality method (Table 4, Fig. 8C). As observed with the Crim Dell Creek biofilm samples, this represented less than 1% of the total biofilm bacterial abundance, and the mortality method resulted in higher error than the other two methods.

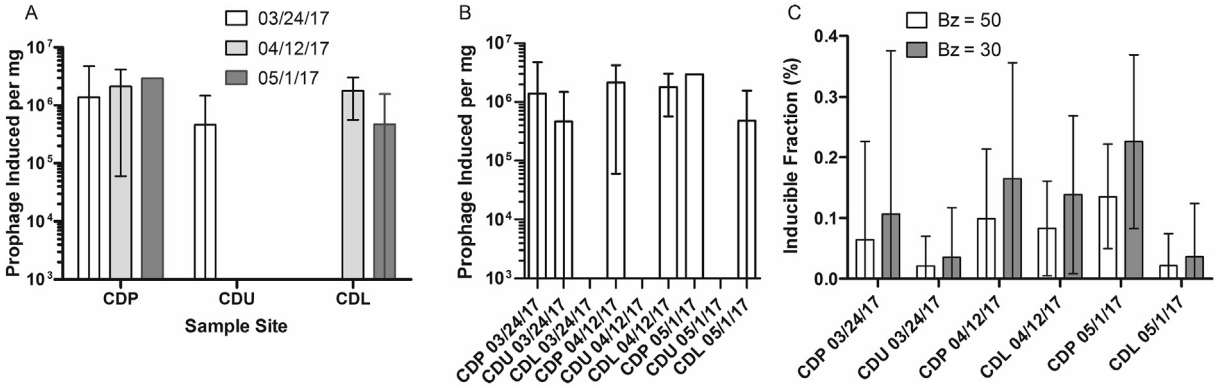

Fig. 7. A) Comparison of the amount of observed prophage induced per sample of natural biofilm. Error bars represent range (N = 2). B) Prophage induction results grouped by sampling site. Error bars represent range (N = 2). C). The inducible fraction according to either a bacterial burst size of 50 and 30. Error bars represent range (N = 2).

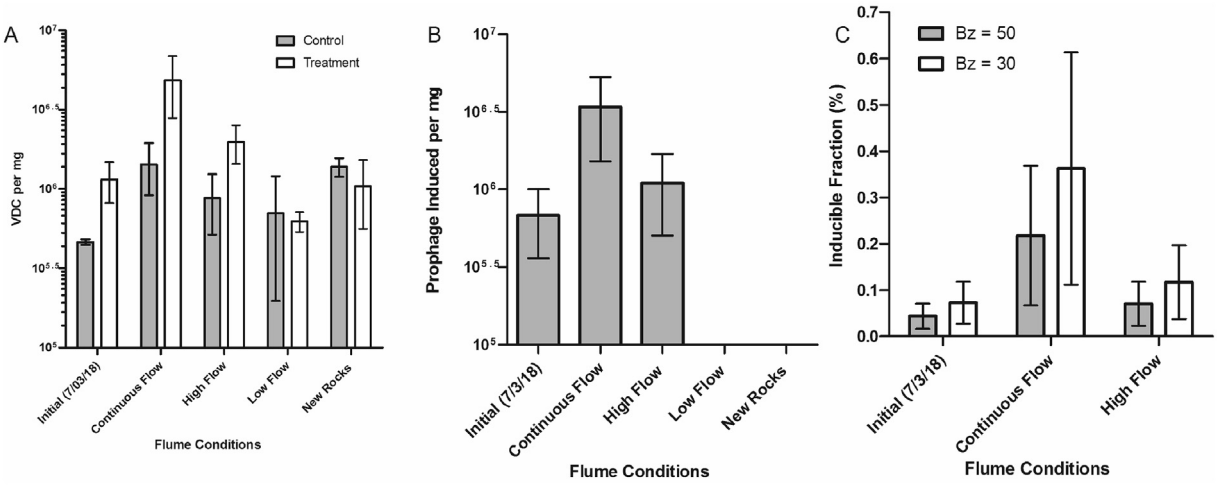

Fig. 8. A) The viral direct count (VDC) comparison between the treatment and control samples. Error bars represent SD (N = 3). C) Number of prophage induced for each of the experimental flumes. Error bars represent SD (N = 3). C) The inducible fraction assuming a burst size of 50 (dark grey bars) or 30 (light grey bars). Error bars represent SD (N = 3).

Table 4
Calculation of Inducible Fraction for experimental flume biofilms Inducible Fraction Calculation.

Flume Condition	Prophage Induced mg^{-1}	$B_Z = 50$	$B_Z = 30$	Mortality Method	Induced B_Z
Initial	$6.82 \times 10^5 \pm 3.21 \times 10^5$	0.044 ± 0.027	0.073 ± 0.046	21.3 ± 22.6	0.102 ± 0.088
Continuous	$3.41 \times 10^6 \pm 1.89 \times 10^6$	0.22 ± 0.15	0.36 ± 0.25	46.4 ± 96.2	0.234 ± 0.457
High Flow	$1.10 \times 10^6 \pm 5.95 \times 10^5$	0.070 ± 0.048	0.12 ± 0.080	55.1 ± 81.5	0.064 ± 0.084

B_z = bacterial burst size; VDC = viral direct count; BDC = bacterial direct count. Results are represented as averages between replicates ± SD (N = 3).

Optimization of RAPD-PCR for biofilm viral concentrates

Only the initial (untreated with nuclease) time point showed evidence that extracellular DNA was present, and one round of cyanase treatment was sufficient to remove extracellular DNA prior to RAPD-PCR (Fig. S1). In all subsequent experiments utilizing RAPD-PCR on biofilm viral concentrates, one round of cyanase treatment was used to remove extracellular DNA prior to amplification. Two rounds of RAPD-PCR were required to generate sufficient DNA for visualization of bands (Fig. S1). PCR inhibition did not appear to be an issue, as positive control bands were clearly amplified (Fig. S1).

Application of RAPD-PCR to compare biofilm viral communities

Triplicate reactions were used to evaluate the reproducibility of the method for analyzing biofilm virus community composition. While replicates grouped together, they did not generate identical banding patterns, indicating some degree of variation across replicate reactions (Fig. 9A). In spite of this within-sample variation, cluster dendrograms indicated a clear progression in biofilm viral community composition over time (Fig. 9B).

Discussion

Viruses have been observed in almost all ecosystems on Earth, but the specific ways in which viruses interact with their hosts and the broader impacts of these interactions have yet to be determined for many ecosystems [10,49,50]. The present work focuses on microbial communities of lotic ecosystems in which the potential roles of viruses are currently unknown. Previous research on virus interactions with biofilms has focused on single-species biofilms and have primarily related findings to medical applications [51,52]. Thus, a main contribution of the present work is to begin to define the ecological roles and interactions of viruses in lotic systems with polymicrobial biofilms [31,38].

Viral abundance

Through epifluorescence microscopy (EFM), evidence of virus like particles (VLPs) was found in all biofilm samples collected from multiple lotic ecosystems (Crim Dell Creek, VA; White Clay Creek, PA; and experimental flumes). Additionally, visual evidence of phage particles was confirmed using transmission electron microscopy. Electron micrographs revealed diverse viral morphologies within biofilm communities (Fig. 6). Collectively, these data suggest that viruses are consistent members of stream biofilm communities, although their mechanism of production is not yet understood. This is important because viruses produced through lytic infections may impact biofilm community composition and nutrient (re)cycling within the biofilm community [9,53]. Beyond lytic production, however, virus particles may be entrained in the biofilm matrix from waters flowing across the biofilm, or viruses may be released through induction of lysogens, which has been shown to occur in some biofilms [54]. Resolving these possibilities should be an important goal of future work in this field, as such efforts would help establish the degree to which viruses may shape biofilm development, maturation, and functionality.

Prophage induction

Due to the toxicity of mitomycin C, samples that do not produce extracellular phage particles often experience rapid declines in both bacterial and viral abundances [29,47]. Thus, similar observations made in the present study were neither unexpected nor unprecedented. It was hypothesized that lysogeny would be prevalent in lotic biofilms because it provides a mechanism for phages to be maintained in the active layer of the biofilm as prophages. The proportion of biofilm samples that tested positive for prophage induction with mitomycin C supported this hypothesis: 6 out of 9 natural biofilm samples (66.7%) and 3 out of 5 samples from biofilms grown in experimental flumes (60%) showed evidence of prophage induction. These findings suggest that temperate phages play some role in bacterial biofilms. Laboratory-scale studies with single species biofilms suggests that prophage induction is an important process in the release of extracellular DNA, a necessary component of the

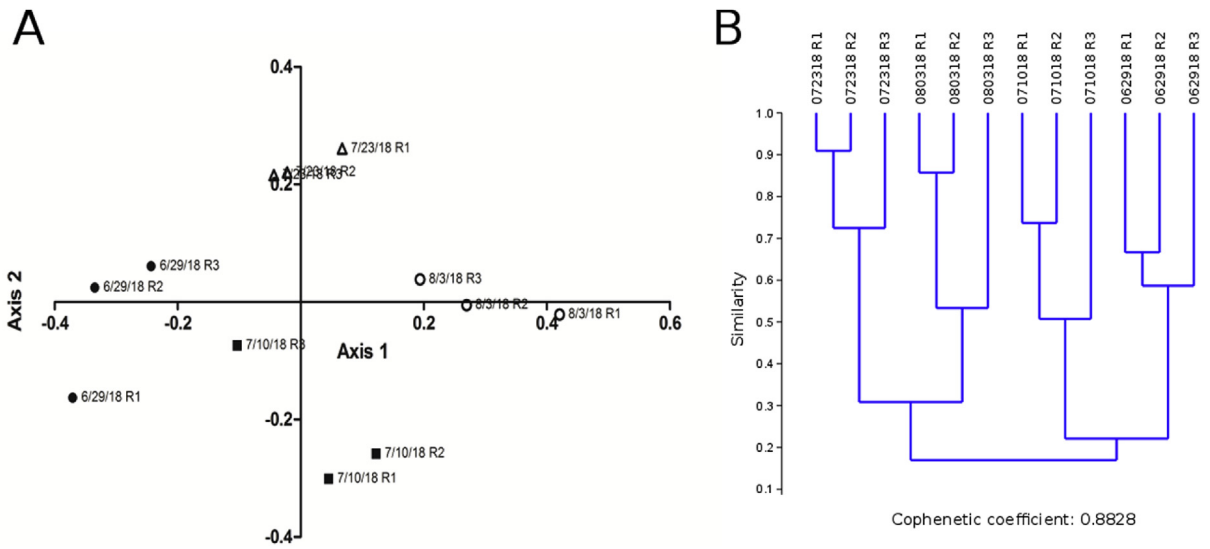

Fig. 9. A) multidimensional scaling (MDS) plot of biofilm virus community RAPD-PCR banding patterns, from samples collected on 06/29/18, 07/10/18, 07/23/18, and 08/03/18 from Flume 1 (High Flow Storm Treatment). B) Cluster dendrogram depicting the similarity of the same viral communities represented in panel A.

biofilm matrix [54–56]. Thus, prophage induction may likewise be an important mechanism for building the biofilm matrix in mixed species lotic biofilms.

Although prophage induction was significant with respect to the number of VLPs in mitomycin C-treated samples relative to untreated controls, only a small percentage of the biofilm bacterial community appeared to induce (Tables 2 and 4). Here we suggest two possible explanations for this contradiction. First, because the samples were mixed-species biofilms, it is possible that a minority of bacterial taxa that make up the biofilm could be producing the majority of phage particles during induction. If these relatively few bacterial taxa are outnumbered by other bacterial taxa that do not induce, then this could explain the significant amount of phage particles being induced despite a small proportion of the bacterial population actually inducing. Alternatively, since the biofilm cuticle and matrix include dead cells, these cells could have been included in the inducible fraction calculations based on epifluorescence microcopy direct counts. While live/dead fluorescent staining approaches have been used to estimate the proportion of viable cells in biofilms, reported values vary widely, from 34% [57] up 100% [58]. Further, a thorough review points out the manifold problems of applying live/dead staining assays to mixed species biofilms [59], emphasizing that the manuals for most live/dead staining kits specify their lack of suitability for natural multispecies biofilm research. Since EFM does not differentiate between live and dead cells in the samples, and commercial live/dead staining kits may not resolve this issue, explaining the unusually small proportion of inducible cells observed in the present study seems an eminent challenge for the future.

Effectiveness of RAPD-PCR

Random amplified polymorphic DNA polymerase chain reaction (RAPD-PCR) has been used in several previous studies to assess viral community composition over time [42,44,46,60]. One aim of this study was to assess the effectiveness of RAPD-PCR use for quantifying changes viral community composition in bacterial biofilms and biofilm samples were analyzed from the high-flow storm flume.

Initial attempts to apply RAPD-PCR to biofilm viral concentrates were unsuccessful, and further testing established that two rounds of RAPD-PCR were necessary to resolve band patterns for most samples. This optimized protocol was then applied to a time series of biofilm viral concentrates obtained from the experimental flume biofilms. A clear temporal progression in viral community composition was observed (Fig. 9). These changes in viral OTUs detected by RAPD-PCR could be reflective of changes in host community succession as the biofilm matured, with the different host community structures supporting different assemblages of viruses. Replicates of a given sample were highly similar (Fig. 9) but most did not meet the conventional similarity cutoff for RAPD-PCR. In previous studies involving RAPD-PCR, identical replicates have been shown to generate 80% or greater similarity in banding patterns [46]. Our results indicated higher than acceptable variability between replicates for RAPD-PCR to be used as a reliable tool for tracking viral community changes in biofilms. Therefore, future work with RAPD-PCR on biofilms should use multiple replicates and determine whether this variability can be constrained. Due to the low costs and high throughput of RAPD-PCR as a means of conducting viral community composition analysis, it is worthwhile to continue refinement of methods that would enable its application to biofilm virus assemblages. Specifically, the use of fluorescently tagged primers and capillary electrophoresis to determine amplified fragment sizes has proven a more effective method than slab gels for characterizing viral community composition in challenging media such as soils [44].

Conclusions

Our results suggest that viruses are relevant members of biofilm communities in freshwater environments throughout all stages of biofilm growth observed in this study. While community-level profiling of biofilm viruses still requires refinement, preliminary assessments suggest temporal changes in biofilm viral communities coupled to biofilm growth and maturation. This, in turn, suggests that viruses are active and participating members of biofilm communities, with the potential to influence community abundance, composition, and functionality with potential implications at the ecosystem level. Inducible prophages were present in ~60% of the biofilm samples tested, again suggesting that prophages may be common and stably maintained in most lotic biofilm communities. Indeed, prophage induction could be an important mechanism in generating the extracellular DNA required for efficient biofilm formation. These data strongly suggest that viruses play important roles in the ecology and development of natural mixed-species biofilms in lotic freshwaters.

Funding

We would like to acknowledge funding from NSF LTERB (DEB-

1557063) and Endowment from Stroud Water Research Center. This research did not receive any specific grant from funding agencies in the public, commercial, or not-for-profit sectors.

Author contributions

KEW, JK, MP and ATP conceived and designed the experiments; ATP, AJD KEW, and RB performed the experiments and collected the data; ATP and KEW analyzed the data; ATP wrote the manuscript; KEW, JK, MP and RB revised and edited the manuscript.

Appendix A. Supplementary data

Supplementary data to this article can be found online at https://doi.org/10.1016/j.bioflm.2019.100016.

References

[1] Suttle CA. Marine viruses — major players in the global ecosystem. Nat Rev Microbiol 2007;5:801–12.
[2] Weinbauer MG, Rassoulzadegan F. Are viruses driving microbial diversification and diversity? Environ Microbiol 2004;6:1–11.
[3] Wommack KE, Colwell RR. Virioplankton: viruses in aquatic ecosystems. Microbiol Mol Biol Rev 2000;64:69–114.
[4] Chibani-Chennoufi S, Bruttin A, Dillmann M-L, Brüssow H. Phage-host interaction: an ecological perspective. J Bacteriol 2004;186:3677–86.
[5] Thingstad TF. Elements of a theory for the mechanisms controlling abundance, diversity, and biogeochemical role of lytic bacterial viruses in aquatic systems. Limnol Oceanogr 2000;45:1320–8.
[6] Azam F, Fenchel T, Field J, Gray J, Meyer-Reil L, Thingstad F. The ecological role of water-column microbes in the sea. Mar Ecol Prog Ser 1983;10:257–63.
[7] Bonilla-Findji O, Malits A, Lefèvre D, Rochelle-Newall E, Lemée R, Weinbauer MG, Gattuso J-P. Viral effects on bacterial respiration, production and growth efficiency: consistent trends in the Southern Ocean and the Mediterranean Sea. Deep Sea Res Part II Top Stud Oceanogr 2008;55:790–800.
[8] Bratbak G, Heldal M, Thingstad TF, Tuomi P. Dynamics of virus abundance in coastal seawater. FEMS Microbiol Ecol 1996;19:263–9.
[9] Fuhrman JA. Marine viruses and their biogeochemical and ecological effects. Nature 1999;399:541–8.
[10] Peduzzi P. Virus ecology of fluvial systems: a blank spot on the map? Biol Rev 2016;91:937–49.
[11] Pal C, Maciá MD, Oliver A, Schachar I, Buckling A. Coevolution with viruses drives the evolution of bacterial mutation rates. Nature 2007;450:1079–81.
[12] Mosig G, Eiserling F. T4 and related phages: structure and development. In: The bacteriophages, calendar. Oxford University Press; 2006. p. 225–67.
[13] Campbell A. General aspects of lysogeny. In: Calendar R, editor. The bacteriophages. New York: Oxford University Press; 2006. p. 66–73.
[14] Miller RV. Marine phages. In: Calendar R, editor. The bacteriophages. New York: Oxford University Press; 2006. p. 534–44.
[15] Russel M, Model P. Filamentous phage. In: Calendar R, editor. The bacteriophages. New York: Oxford University Press; 2006. p. 146–60.
[16] Ackermann H-W, DuBow MS. Viruses of prokaryotes general properties of bacteriophages. Boca Raton, FL: CRC Press, Inc.; 1987.
[17] Roberts JW, Devoret R. Lysogenic induction. In: Hendnx RW, editor. Lambda II. NY: Cold Spring Harbor Labrotory; 1983. p. 123–44. Cold Spring Harbor.
[18] Goldenfeld N, Woese C. Biology's next revolution. Nature 2007;445. 369–369.
[19] Lenski RE, Levin BR. Constraints on the coevolution of bacteria and virulent phage: a model, some experiments, and predictions for natural communities. Am Nat 1985;125:585–602.
[20] Replicon J, Frankfater A, Miller RV. A continuous culture model to examine factors that affect transduction among Pseudomonas aeruginosa strains in freshwater environments. Appl Environ Microbiol 1995;61:3359–66.
[21] Saye DJ, Ogunseitan O, Sayler GS, Miller RV. Potential for transduction of plasmids in a natural freshwater environment: effect of plasmid donor concentration and a natural microbial community on transduction in Pseudomonas aeruginosa. Appl Environ Microbiol 1987;53:987–95.
[22] Wilcox R, Fuhrman J. Bacterial-viruses in coastal seawater - lytic rather than lysogenic production. Mar Ecol Prog Ser 1994;114:35–45.
[23] Weinbauer MG, Brettar I, Höfle MG. Lysogeny and virus-induced mortality of bacterioplankton in surface, deep, and anoxic marine waters. Limnol Oceanogr 2003;48:1457–65.
[24] Williamson SJ, Cary SC, Williamson KE, Helton RR, Bench SR, Winget D, Wommack KE. Lysogenic virus–host interactions predominate at deep-sea diffuse-flow hydrothermal vents. ISME J 2008;2:1112–21.
[25] Williamson KE, Radosevich M, Smith DW, Wommack KE. Incidence of lysogeny within temperate and extreme soil environments. Environ Microbiol 2007;9:2563–74.
[26] Mei ML, Danovaro R. Virus production and life strategies in aquatic sediments. Limnol Oceanogr 2004;49:459–70.
[27] Long A, McDaniel LD, Mobberley J, Paul JH. Comparison of lysogeny (prophage induction) in heterotrophic bacterial and Synechococcus populations in the Gulf of Mexico and Mississippi River plume. ISME J 2008;2:132–44.
[28] McDaniel L, Houchin LA, Williamson SJ, Paul JH. Lysogeny in marine synechococcus. Nature 2002;415:496.
[29] Williamson SJ, Houchin LA, McDaniel L, Paul JH. Seasonal variation in lysogeny as depicted by prophage induction in Tampa Bay, Florida. Appl Environ Microbiol 2002;68:4307–14.
[30] Williamson SJ, Paul JH. Nutrient stimulation of lytic phage production in bacterial populations of the Gulf of Mexico. Aquat Microb Ecol 2004;36:9–17.
[31] Battin TJ, Besemer K, Bengtsson MM, Romani AM, Packmann AI. The ecology and biogeochemistry of stream biofilms. Nat Rev Microbiol 2016;14:251–63.
[32] Romaní AM, Fund K, Artigas J, Schwartz T, Sabater S, Obst U. Relevance of polymeric matrix enzymes during biofilm formation. Microb Ecol 2008;56:427–36.
[33] Raymond PA, Hartmann J, Lauerwald R, Sobek S, McDonald C, Hoover M, Butman D, Striegl R, Mayorga E, Humborg C, et al. Global carbon dioxide emissions from inland waters. Nature 2013;503:355–9.
[34] O'Toole G, Kaplan HB, Kolter R. Biofilm formation as microbial development. Annu Rev Microbiol 2000;54:49–79.
[35] Beveridge TJ, Makin SA, Kadurugamuwa JL, Li Z. Interactions between biofilms and the environment. FEMS Microbiol Rev 1997;20:291–303.
[36] Hansen SK, Rainey PB, Haagensen JAJ, Molin S. Evolution of species interactions in a biofilm community. Nature 2007;445:533–6.
[37] Besemer K, Singer G, Quince C, Bertuzzo E, Sloan W, Battin TJ. Headwaters are critical reservoirs of microbial diversity for fluvial networks. Proc R Soc Lond B Biol Sci 2013;280:20131760.
[38] Findlay S. Stream microbial ecology. J North Am Benthol Soc 2010;29:170–81.
[39] Watnick P, Kolter R. Biofilm, city of microbes. J Bacteriol 2000;182:2675–9.
[40] Battin TJ, Kaplan LA, Denis Newbold J, Hansen CME. Contributions of microbial biofilms to ecosystem processes in stream mesocosms. Nature 2003;426:439–42.
[41] Carreira C, Staal M, Middelboe M, Brussaard CPD. Counting viruses and bacteria in photosynthetic microbial mats. Appl Environ Microbiol 2015;81:2149–55.
[42] Hardbower DM, Dolman JL, Glasner DR, Kendra JA, Williamson KE. Optimization of viral profiling approaches reveals strong links between viral and bacterial communities in a eutrophic freshwater lake. Aquat Microb Ecol 2012;67:59–76.
[43] Filée J, Tétart F, Suttle CA, Krisch HM. Marine T4-type bacteriophages, a ubiquitous component of the dark matter of the biosphere. Proc Natl Acad Sci 2005;102:12471–6.
[44] Narr A, Nawaz A, Wick LY, Harms H, Chatzinotas A. Soil viral communities vary temporally and along a land use transect as revealed by virus-like particle counting and a modified community fingerprinting approach (fRAPD). Front Microbiol 2017;8.
[45] Marston MF, Amrich CG. Recombination and microdiversity in coastal marine cyanophages. Environ Microbiol 2009;11:2893–903.
[46] Winget DM, Wommack KE. Randomly amplified polymorphic DNA PCR as a tool for assessment of marine viral richness. Appl Environ Microbiol 2008;74:2612–8.
[47] Cochran PK, Paul JH. Seasonal abundance of lysogenic bacteria in a subtropical estuary. Appl Environ Microbiol 1998;64:2308–12.
[48] Hammer Ø, Harper D, Ryan P. PAST: paleontological statistics software package for education and data analysis. Palaeontol Electron 2001;1–9.
[49] Hansen MF, Svenningsen SL, Røder HL, Middelboe M, Burmølle M. Big impact of the tiny: bacteriophage–bacteria interactions in biofilms. Trends Microbiol 2019;27:739–52.
[50] Williamson KE, Fuhrmann JJ, Wommack KE, Radosevich M. Viruses in soil ecosystems: an unknown quantity within an unexplored territory. Annu Rev Virol 2017;4:201–19.
[51] Abdallah M, Benoliel C, Drider D, Dhulster P, Chihib N-E. Biofilm formation and persistence on abiotic surfaces in the context of food and medical environments. Arch Microbiol 2014;196:453–72.
[52] Khoury AE, Lam K, Ellis B, Costerton JW. Prevention and control of bacterial infections associated with medical devices. ASAIO J Am Soc Artif Intern Organs 1992;38:M174–8. 1992.
[53] Schwalbach MS, Hewson I, Fuhrman JA. Viral effects on bacterial community composition in marine plankton microcosms. Aquat Microb Ecol 2004;34:117–27.
[54] Carrolo M, Frias MJ, Pinto FR, Melo-Cristino J, Ramirez M. Prophage spontaneous activation promotes DNA release enhancing biofilm formation in Streptococcus pneumoniae. PLoS One 2010;5. e15678.
[55] Gödeke J, Paul K, Lassak J, Thormann KM. Phage-induced lysis enhances biofilm formation in Shewanella oneidensis MR-1. ISME J 2011;5:613–26.
[56] Shen M, Yang Y, Shen W, Cen L, McLean JS, Shi W, Le S, He X. A linear plasmid-like prophage of actinomyces odontolyticus promotes biofilm assembly. Appl Environ Microbiol 2018;84. UNSP e01263-18.
[57] Tawakoli PN, Al-Ahmad A, Hoth-Hannig W, Hannig M, Hannig C. Comparison of different live/dead stainings for detection and quantification of adherent microorganisms in the initial oral biofilm. Clin Oral Investig 2013;17:841–50.
[58] Shen Y, Stojicic S, Haapasalo M. Bacterial viability in starved and revitalized biofilms: comparison of viability staining and direct culture. J Endod 2010;36:1820–3.
[59] Netuschil L, Auschill TM, Sculean A, Arweiler NB. Confusion over live/dead stainings for the detection of vital microorganisms in oral biofilms - which stain is suitable? BMC Oral Health 2014;14:2.
[60] Williamson KE, Harris JV, Green JC, Rahman F, Chambers RM. Stormwater runoff drives viral community composition changes in inland freshwaters. Front Microbiol 2014;5.